EARTHQUAKE ENGINEERING AND STRUCTURAL DYNAMICS
Earthquake Engng Struct. Dyn. 2003; **32**:999–1020 (DOI: 10.1002/eqe.259)

System identification of instrumented bridge systems

Yalin Arici and Khalid M. Mosalam*,†

Department of Civil and Environmental Engineering, University of California, 721 Davis Hall, Berkeley, CA 94720-1710, U.S.A.

SUMMARY

Several recorded motions for seven bridge systems in California during recent earthquakes were analysed using parametric and non-parametric system identification (SI) methods. The bridges were selected considering the availability of an adequate array of accelerometers and accounting for different structural systems, materials, geometry and soil types. The results of the application of SI methods included identification of modal frequencies and damping ratios. Excellent fits of the recorded motion in the time domain were obtained using parametric methods. The multi-input/single-output SI method was a suitable approach considering the instrumentation layout for these bridges. Use of the constructed linear filters for prediction purposes was also demonstrated for three bridge systems. Reasonable prediction results were obtained considering the various limitations of the procedure. Finally, the study was concluded by identifying the change of the modal frequencies and damping of a particular bridge system in time using recursive filters. Copyright © 2003 John Wiley & Sons, Ltd.

KEY WORDS: autoregressive moving average; earthquake data; instrumented bridges; recursive filters; system identification

BACKGROUND

The system identification (SI) of structures has been an important tool in the last two decades to determine the vibration characteristics of structural systems. Numerous works have been conducted on building systems. In this paper, no attempt is made to review the literature on buildings. Instead, the focus of this concise literature review is on the identification and evaluation techniques performed on bridge structures. A short review of previous research on civil engineering systems using recursive filters is also presented.

Prior to 1999, there were 54 instrumented bridges in California, 47 of which were instrumented in the last decade. These instruments were installed and maintained by the

* Correspondence to: Khalid M. Mosalam, Department of Civil and Environmental Engineering, University of California, 721 Davis Hall, Berkeley, CA 94720-1710, U.S.A.
† E-mail: mosalam@ce.berkeley.edu

Contract/grant sponsor: California Strong Motion Instrumentation Program; Contract/grant number: 1098-714.

Received 29 October 2001
Revised 26 April 2002
Accepted 30 August 2002

California Strong Motion Instrumentation Program (CSMIP). A complete list of instrumented bridges can be found in Hipley *et al.* [1]. One of the oldest extensively instrumented bridges is the El Centro Highway 8/Meloland overpass which was investigated by several researchers, e.g. Werner *et al.* [2, 3] and Wilson and Tan [4]. In these investigations, modal properties were determined using single-input/single-output and multi-input/multi-output methods.

Data recorded from instrumented bridges were used by several researchers for different purposes. Wilson [5] used the recordings from the San Juan Bautista 156/101 overpass to evaluate its seismic response. On the other hand, Safak [6] used data from this bridge for small earthquakes to predict the response of a larger one. Levine and Scott [7] used the ground motion recordings for verification of a bridge foundation model. Fenves and Desroches [8] evaluated the response of the Interstate 5/Route 14 interchange using non-parametric and parametric SI techniques. The Vincent Thomas suspension bridge was studied by Abdel-Ghaffar *et al.* [9] to estimate the modal properties from ambient vibration and Whittier earthquake recordings and by Lus *et al.* [10] using Eigen System Realization Algorithm and Observer/Kalman Filter Identification. One of the unique studies to investigate the effects of vertical earthquake motions on highway bridges was conducted by Saadeghvaziri and Foutch [11] using data from the Rio Dell–Highway 101/Painter Street overpass.

Computational models were developed by several researchers to predict the vibration characteristics of instrumented bridges. The computational results were usually compared with the recorded data in the time or frequency domains. The Hayward BART elevated section was studied by Tseng *et al.* [12] and the results included suggested mass and stiffness coupling effects due to the massive Hayward BART station and the continuity of the railing, respectively. Dumbarton bridge was studied by Fenves *et al.* [13] pointing out the importance of articulations and longitudinal constraints at hinges. The Colton I10/215 Interchange bridge system was studied by Desroches and Fenves [14], who developed computational models with detailed modelling of intermediate hinges to compare the analytical results to recorded responses. The Rio Dell–Highway 101/Painter Street overpass was studied by Goel and Chopra [15] to estimate the stiffness of the abutments and by McCallen and Romstadt [16] using detailed finite-element modelling. For design evaluation, Tsai *et al.* [17] studied Caltrans seismic evaluation procedures of bridge structures using five short-span bridges and showed consistency between the code estimation and the recorded data.

Several studies for analysing recorded data from bridges not in California were also conducted. Chaudhary *et al.* [18] used ground motion recordings from the Kobe earthquake to determine vibration properties of two base-isolated bridges in Japan. Loh and Lee [19] assessed the properties of the New Lian River bridge in Taiwan using weak and strong ground excitations by conducting multi-input/single-output SI.

Several references include reviews of parametric analysis using discrete time filters for linear structural systems, e.g. Safak [20], Fenves and Desroches [8] and Glaser [21]. Recently, the SI methods were focused on monitoring the changes in non-linear systems. Recursive filters are instrumental in that respect. Shinozuka and Ghanem [22] discussed the application of a number of recursive SI methods on structural systems with emphasis on use, applicability and reliability of the methods. Loh and Lin [23] used two types of recursive filter realizations on seismic response data of buildings. More recently, the application of recursive filters for monitoring the change of soil behaviour was given by Glaser and Baise [24].

OBJECTIVES AND LIMITATIONS

The primary objectives of the study can be summarized by the following:

- Application of the SI methodologies to a broad sample of bridges and earthquake data.
- Determination of the modal frequencies of the bridge systems and the corresponding damping ratios using linear filters.
- Examination of the prediction capabilities of the developed linear models.
- Application of recursive filters for estimating the change of modal frequencies and damping ratios during strong shaking.

Notable limitations of the study include:

- Inclusion of only prestressed and reinforced concrete bridge systems.
- Use of only relatively small earthquake events for some of the considered bridges due to lack of strong motion data.
- Inherent deficiency of the used practical multi-input/single-output SI method in identification of mode shapes.

SELECTED BRIDGES AND OBJECTIVES

The selected bridges are presented in Figure 1 with structural information and earthquake data listed in Tables I and II, respectively. The criterion for choosing these bridges was to have a representative sample of commonly used bridge systems in California. These bridges had different characteristics including: material (reinforced concrete (RC) versus prestressed concrete (PC)), bent types (single-column versus multiple-columns), number of spans (2–9 spans), section types (box girders with different number of cells), soil properties (soft versus stiff), structural systems (continuous versus simply supported), and orientation (straight, skewed and curved). Moreover, the availability of a sufficient number of installed accelerometers, for successful SI, governed the choice of the bridges.

METHODOLOGY

The total acceleration $\ddot{\mathbf{u}}_T$ of a multi-degrees-of-freedom system is given by

$$\ddot{\mathbf{u}}_T = \ddot{\mathbf{u}}_r + [\mathbf{I}]\ddot{\mathbf{u}}_g \tag{1}$$

where $\ddot{\mathbf{u}}_r$ and $\ddot{\mathbf{u}}_g$ are vectors of relative structural acceleration and the earthquake (ground) acceleration components, respectively, and $[\mathbf{I}]$ is the system influence coefficient matrix, representing the displacement vectors from a unit support movement in the different directions of earthquake components. Using modal equations [25] and classical damping, $\ddot{\mathbf{u}}_r(t)$ with time t can be expressed according to

$$\ddot{\mathbf{u}}_r(t) = [\mathbf{\Phi}]\ddot{\mathbf{X}}(t) = \sum_{i=1}^{m} \boldsymbol{\varphi}_i \ddot{X}_i(t) \tag{2}$$

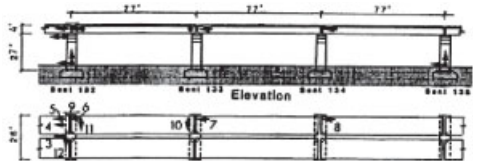

(a) Hayward BART elevated section

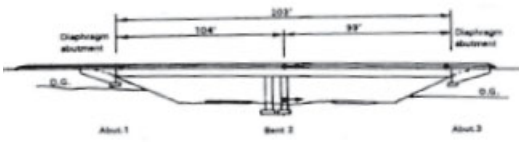

(b) Lake Crowley-Highway 395 bridge

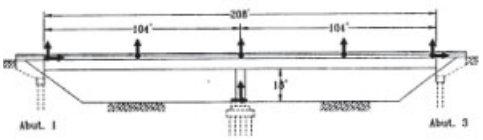

(c) El Centro Highway 8/Meloland overpass

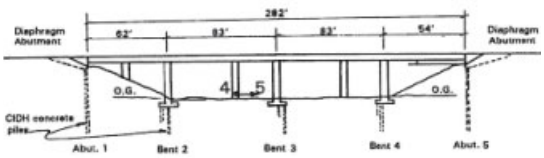

(d) Ridgecrest-Highway 580/13 Interchange

(e) Rio Dell–Highway 101/Painter St. overpass

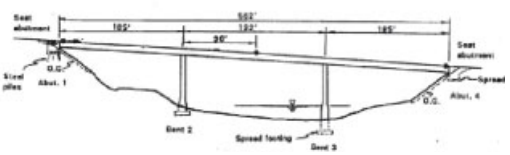

(f) Truckee-I80/Truckee River bridge

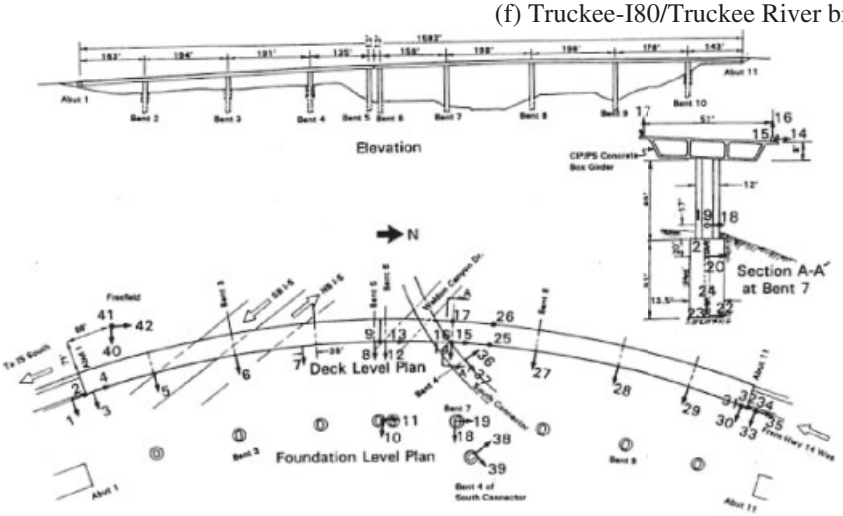

(g) Sylmar I5/14 Interchange

Figure 1. Investigated bridge systems ($1' = 30.48$ cm).

$$\ddot{X}_i(t) + 2\xi_i\omega_i\dot{X}_i(t) + \omega_i^2 X_i(t) = -M_i^{-1}\mathbf{L}_i\ddot{\mathbf{u}}_g(t) \tag{3}$$

$$M_i = \boldsymbol{\varphi}_i^{\mathrm{T}}[\mathbf{M}]\boldsymbol{\varphi}_i \quad \text{and} \quad \mathbf{L}_i = \boldsymbol{\varphi}_i^{\mathrm{T}}[\mathbf{M}][\mathbf{I}] \tag{4}$$

where $[\boldsymbol{\Phi}]$ and $\ddot{\mathbf{X}}(t)$ are the $m \times m$ modal matrix and the generalized response vector, respectively, $\boldsymbol{\varphi}_i$ and $\ddot{X}_i(t)$ representing the ith normal mode vector and the corresponding generalized response, respectively, ξ_i, ω_i, and M_i are the ith modal damping, frequency and mass,

Table I. Selected bridge information ($1' = 30.48$ cm).

Bridge	Structural system	Spans
Hayward BART elevated section	Simply supported PC twin beams on RC single columns with double cantilevers	3 @ 77′
Lake Crowley–Highway 395 bridge	Continuous RC 5-cell box girder on abutments and a 2-column bent	2 @ 104′ & 99′
El Centro Highway 8/ Meloland overpass	Monolithic continuous RC 3-cell box girder on abutments and a single column bent	2 @ 104′
Rio Dell–Highway 101/ Painter St. overpass	Continuous PC 6-cell box girder on abutments and a 2-column bent	2 @ 119′ & 146′
Ridgecrest–Highway 580/13 Interchange	Continuous RC 5-cell box girder on abutments and a 2-column bent	4 @ 62′, 83′, 83′ & 54′
Truckee-I80/Truckee River bridge	Continuous PC 3-cell box girder on inverted A-shaped column bents	3 @ 185′, 192′ & 185′
Sylmar I5/14 Interchange	Continuous PC 3-cell box girder on single column bents with an expansion joint	9 @ 135′ to 198′

respectively, $\mathbf{L}_i$ is the ith row vector of the generalized influence factors for support motions, and [**M**] is the mass matrix. Note that the superscript dots indicate time differentiation and superscript T indicates transpose. In the frequency domain, the solution of Equation (3) is obtained using the Laplace transform as follows:

$$\bar{X}_i(s) = -M_i^{-1}\mathbf{L}_i\bar{\ddot{\mathbf{u}}}_g(s)/(s^2 + 2\xi_i\omega_i s + \omega_i^2) \tag{5}$$

From the above equations, one obtains

$$\bar{\ddot{\mathbf{u}}}_T(s) = \mathbf{H}(s)\bar{\ddot{\mathbf{u}}}_g(s) \quad \text{where } \mathbf{H}(s) = \sum_{i=1}^{m} \frac{2\xi_i\omega_i s + \omega_i^2}{s^2 + 2\xi_i\omega_i s + \omega_i^2} M_i^{-1}\boldsymbol{\varphi}_i\mathbf{L}_i \tag{6}$$

Non-parametric identification

Transfer function estimates (TFE) are used for obtaining system modal frequencies. For stationary input signals, the TFE is defined in either of the following:

$$H_1(i\omega) = S_{xy}(\omega)/S_{xx}(\omega) \quad \text{and} \quad H_2(i\omega) = S_{yy}(\omega)/S_{yx}(\omega) \tag{7}$$

where S_{xx} and S_{yy} are the auto-spectra which are the Fourier transform of the autocorrelations of input signal x and output signal y, respectively, and $S_{xy} = S_{yx}^*$ (superscript * indicates complex conjugate) is the cross-spectrum which is the Fourier transform of the cross-correlation of x with y. It is known that H_1 and H_2 estimates are more susceptible to input noise and output noise, respectively. Accordingly, the results for the TFE were based on the H_2 form of Equation (7).

Table II. Earthquake data.

Bridge	Date	Free field/Deck Max. Hz. Acc. (g)
Hayward BART elevated section	10/17/1989	0.160/0.508
Lake Crowley–Highway 395 bridge	06/08/1998	0.200/0.244
	06/14/1987	0.231/0.405
	05/15/1999	0.092/0.269
El Centro Highway 8/Meloland overpass	04/09/2000	0.043/0.174
	06/14/2000(1)	0.013/0.044
	06/14/2000(2)	0.011/0.038
Rio Dell–Highway 101/Painter Street overpass	11/21/1986	0.432/0.399
	07/31/1987	0.141/0.335
	04/25/1992	0.543/1.089
Ridgecrest–Highway 580/13 Interchange	05/06/1997	0.005/0.016
	03/05/1998	0.019/0.077
Truckee-I80/Truckee River bridge	10/30/1998	0.088/0.172
	12/02/2000	0.020/0.045
	08/10/2001	0.020/0.042
Sylmar I5/14 Interchange	04/11/1999	0.011/0.066
	10/16/1999	0.019/0.052

Parametric identification

TFE provides accurate identification of the frequency and mode shapes only for the first few modes. A more accurate alternative is the use of linear discrete time models, which yield both frequency and damping information. The typical single-input/single-output *discrete* time filter is expressed as

$$y(t) = b_0 x(t) + b_1 x(t-1) + \cdots - a_1 y(t-1) - a_2 y(t-2) - \cdots \tag{8}$$

where $x(t)$ and $y(t)$ are the input and output of the system at time t, respectively. The input series 'b' coefficients are the causal moving average (MA) process with order n_b, and the output series 'a' coefficients are the non-causal auto-regressive (AR) process with order n_a. Taking the Fourier transform of the above expression and applying the Z-transform gives the following transfer function for this discrete system:

$$H(\omega) = Y_\omega / X_\omega = (b_0 + b_1 z + b_2 z^2 + \cdots + b_{n_b} z^{n_b}) / (1 + a_1 z + a_2 z^2 + \cdots + a_{n_a} z^{n_a}) \tag{9}$$

Various forms of the ARMA method exist in the literature with the general format of a multi-input/single-output system given by the polynomial

$$A(z) y(t) = \sum_{i=1}^{NI} [B_i(z)/F_i(z)] x_i(t - \delta_i) + [C(z)/D(z)] e(t) \tag{10}$$

where A, B, C, D and F are polynomials in terms of the shift operator z to define various system properties, $e(t)$ is the model prediction error, and δ is the time delay in the input.

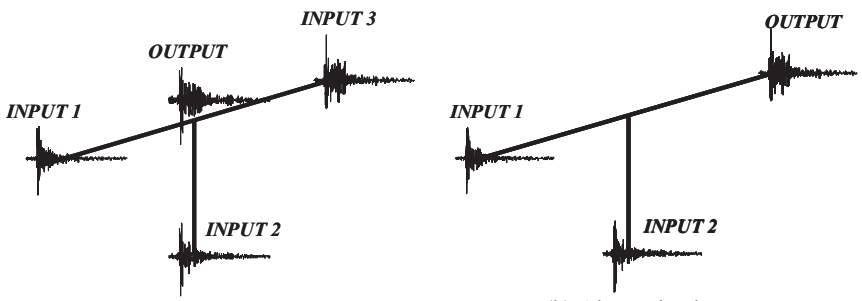

(a) Typical (T) layout (b) Alternative layout

Figure 2. Layout of accelerometers for SI.

The summation in Equation (10) is performed for the number of inputs NI. The output error (OE) and the auto-regressive extended (ARX) models were selected in this study because they are widely used in SI of structures. In Equation (10), the OE model corresponds to the case of A, C and D being unity, while the ARX model corresponds to C, D and F being unity. The other parameters are estimated using least square minimization of the last term in Equation (10) [26].

The modal frequencies of the dynamic system can be obtained from the poles of the transfer function between the different inputs and the output. The poles are the roots of the denominator of Equation (9), z_i, which exist in $n_a/2$ complex conjugate pairs. These can be transformed to the poles of the transfer function defined in Equation (6) using the transformation $s_i = \ln(z_i)/\Delta t$ where Δt is the sampling interval with total number of time steps N. Subsequently, one obtains the modal frequencies $\omega_i = \sqrt{s_i \times s_i^*}$ and damping ratios $\xi_i = -\mathrm{Re}(s_i)/\omega_i$ for the considered $n_a/2$ modes.

The simulated and recorded outputs are usually compared to assess the quality of the models. This is conducted using the normalized mean square error, J, defined by Werner *et al.* [2] and referred to in the following analysis as the *simulation error*:

$$J = \sum_{i=1}^{N} (y_i - y_i^{\mathrm{sim}})^2 \Big/ \sum_{i=1}^{N} (y_i)^2 \tag{11}$$

where y_i and y_i^{sim} are the actual recording from the structure and the simulated model output, respectively. A value of J less than 0.1 corresponds to an excellent model, whereas J in the range of 0.1–0.5 corresponds to an adequate model. Time history fits with J greater than 0.5 are poor and the corresponding results are disregarded.

All selected bridges, except BART, were analysed using the multi-input/single-output approach with the accelerometers layout given by Figure 2(a). System identification that considers multiple-output degrees of freedom is more advantageous as it provides more insights into bridge behaviour (i.e. modal shapes). On the other hand, the study was limited to single-output for several reasons, including, (i) The study focuses on the estimation of frequencies and damping ratios. (ii) The study aims at developing a general method with a simple sub-structuring idea which is applicable to generic bridge systems with common instrumentation pattern, see Figure 2(a). (iii) The available geometry of bridges and number and layout of

sensors on the considered bridge systems are more suitable for the single-output approach. (iv) Simplicity and practicality of single-output methods are essential especially when dealing with seven different systems as in the present study.

An alternative layout of accelerometers is shown in Figure 2(b), which is adopted for the SI of one bridge system, as discussed later. In the BART elevated segment, the structural system was not suitable for multi-input/single-output analysis, instead single-input/single-output was used. For the OE models, the determined frequencies and damping ratios were for each of the input/output pairs. The frequencies and damping ratios between the ground input 2 (see Figure 2) and the superstructure output were selected to be the best candidate for estimating the system vibration characteristics. For the ARX models, a single group of frequencies and damping ratios were determined from the whole structural system.

Recursive parametric identification

The used recursive filter algorithm is an online modification of the ARX method, which updates the model parameters as more data becomes available. In this case, the linear regression model in Equation (8) is expressed as

$$y(t) = \mathbf{\Psi}(t)^{\mathrm{T}}\mathbf{\Theta}_0(t) + e(t) \tag{12}$$

with 'true' parameters $\mathbf{\Theta}_0(t)$ and prediction error $e(t)$. For several inputs $x_1, x_2, \ldots$, the regression vector $\mathbf{\Psi}(t)$ is

$$\mathbf{\Psi}(t) = [-y(t-1), \ldots, -y(t-n_a), x_1(t-1), \ldots, x_1(t-n_b), x_2(t-1), \ldots, x_2(t-n_b), \ldots]^{\mathrm{T}} \tag{13}$$

The generic Kalman filter algorithm, given below, with gain vector $\mathbf{K}(t)$ was used to estimate the change of the model parameters in time.

$$\hat{\mathbf{\Theta}}(t) = \hat{\mathbf{\Theta}}(t-1) + \mathbf{K}(t)(y(t) - \hat{y}(t)) \tag{14}$$

$$\hat{y}(t) = \mathbf{\Psi}(t)^{\mathrm{T}}\hat{\mathbf{\Theta}}(t-1) \tag{15}$$

$$\mathbf{K}(t) = \mathbf{Q}(t)\mathbf{\Psi}(t) \tag{16}$$

$$\mathbf{Q}(t) = \mathbf{P}(t-1)/(R_2 + \mathbf{\Psi}(t)^{\mathrm{T}}\mathbf{P}(t-1)\mathbf{\Psi}(t)) \tag{17}$$

$$\mathbf{P}(t) = \mathbf{P}(t-1) + \mathbf{R}_1 - \mathbf{P}(t-1)\mathbf{\Psi}(t)\mathbf{\Psi}(t)^{\mathrm{T}}\mathbf{P}(t-1)/(R_2 + \mathbf{\Psi}(t)^{\mathrm{T}}\mathbf{P}(t-1)\mathbf{\Psi}(t)) \tag{18}$$

The above algorithm is entirely specified by the drift matrix $\mathbf{R}_1$, the variance of the noise R_2, the initial values of the matrix $\mathbf{P}(0)$ and parameters vector $\hat{\mathbf{\Theta}}(0)$, and the data sequences $y(t), x_1(t), x_2(t), \ldots$.

Several variations of the above adaptive filtering algorithm exist depending on the error criteria. The most popular one is the 'forgetting factor' algorithm where the normalized prediction error is factored to reduce the effect of data further back in time. In this case, it is required to minimize $\sum_{i=1}^{t} \lambda^{t-i} e(i)^2$ with Equation (17) replaced by

$$\mathbf{Q}(t) = \mathbf{P}(t) = \mathbf{P}(t-1)/(\lambda + \mathbf{\Psi}(t)^{\mathrm{T}}\mathbf{P}(t-1)\mathbf{\Psi}(t)) \tag{19}$$

The forgetting factor λ in the range of 0.97–0.995 is usually recommended [26], with values close to 0.99 for structural systems [22]. A small λ corresponds to a smaller effect of past data on the current model. Accordingly, the choice of λ depends on the rate by which the system changes. It should be noted that $\lambda = 1$ converges to the ARX linear model estimation.

The recursive filter algorithms applied to non-linear systems are known to yield better time history fits with low model orders [24]. The forgetting factor algorithm is also known to be robust with scarce dependency on initial values of the parameters and relative ease of use compared with other algorithms [22]. One of the variations of the forgetting factor algorithm involves changing λ in time to better represent the rate of change of the system. In this study, the forgetting factor algorithm with constant λ was adopted for the recursive SI of the Rio Dell–Highway 101/Painter Street overpass.

LINEAR SYSTEM IDENTIFICATION

Results and discussions

The SI results of the first six bridges are given in Table III. For consistency, the reported results for all the analysed bridges correspond to the lowest simulation error. The results for the Hayward BART elevated section are presented for the longitudinal and transverse directions separately. Although the fundamental frequency in the longitudinal direction was 1.00 Hz, the third mode corresponding to 3.40 Hz was the dominant mode because of the high mass coupling provided by the nearby Hayward BART station and by the stiffness coupling due to the continuous railing on the structure. The frequency values obtained from SI are very close to the values estimated by Tseng *et al.* [12].

Slightly different values of the fundamental frequency of the Lake Crowley–Highway 395 bridge were obtained from the analysed earthquakes. The value of 4.80 Hz from the ARX method was chosen as the fundamental frequency.

The fundamental frequency of the El Centro–Highway 8/Meloland overpass was determined to be 3.22 Hz based on the ARX method. As the bridge is monolithic with the abutments, the mode shapes involved embankment movements. Werner *et al.* [2] determined modal frequencies of 2.50 and 3.20 Hz for the case involving embankment movement, and 3.70 Hz for the case involving only superstructure movement. It is worth mentioning that the analysed ground motions in the present study were much smaller than those used by Werner *et al.* [2], which may explain the absence of the 2.5 Hz mode in the present analysis. Accordingly, it is concluded that the mobilization of embankments is a strong factor affecting the behaviour of this bridge, which is strongly correlated with the degree of shaking experienced at the site. An example of the time history fit for transverse acceleration (E–W) recording at the bent of this bridge (channel 7) is shown in Figure 3 where an excellent fit is clear.

The data from the first two events of the Rio Dell–Highway 101/Painter Street overpass was analysed and the fundamental frequency was determined to be 3.50 Hz from the first event. This estimation is very close to the results of a previous study on this system by Maroney *et al.* [27] establishing 3.57 Hz as the fundamental transverse frequency. For the third earthquake, the SI results were significantly different from those of the first two events. This was expected since the maximum acceleration of the superstructure reached 1.1 g during the third event indicating possible change in the system properties. This change is addressed later in the paper using recursive filters.

Table III. Results of linear SI.

Bridge	Earthquake date	Mode #	TFE	OE		ARX	
			ω (Hz)	ω (Hz)	ξ (%)	ω (Hz)	ξ (%)
BART (Long.)	10/17/1989	1	1.00	—	—	—	—
		2	1.90	2.07	2.12	—	—
		3	3.40	3.61	1.08	—	—
BART (Trans.)	10/17/1989	1	1.80	1.67	6.20	1.67	6.88
		2	3.60	3.60	39.49	3.69	5.24
Lake Crowley—Highway 395 bridge	06/08/1998	1	4.90	5.08	1.07	5.00	13.23
		2	5.60	5.65	0.73	5.79	4.97
	06/14/1998	1	4.60	4.87	9.67	4.80	8.74
		2	5.45	5.51	8.57	6.15	4.38
	05/15/1999	1	4.60	4.73	2.73	4.74	8.92
		2	5.40	5.33	5.77	5.64	3.86
El Centro Hwy 8/Meloland overpass	04/09/2000	1	3.10	3.08	4.36	3.22	5.40
		2	3.50	3.64	8.84	3.63	6.45
	06/14/2000(1)	1	3.40	3.33	24.27	3.39	24.69
		2	—	3.86	5.18	3.85	3.25
	06/14/2000(2)	1	3.40	3.30	3.12	3.36	12.25
		2	4.00	3.96	5.21	3.94	3.68
Rio Dell–Highway 101/Painter Street overpass	11/21/1986	1	3.55	3.50	13.79	3.50	23.68
		2	—	4.22	5.33	4.63	6.16
	07/31/1987	1	3.35	3.33	0.66	3.67	8.71
		2	4.35	4.86	2.1	4.74	6.44
	04/25/1992	1	2.95	—	—	3.14	10.53
		2	4.65	—	—	4.33	6.43
Ridgecrest Interchange	05/06/1997	1	3.57	3.54	1.31	3.68	1.76
	03/05/1998	1	3.33	3.39	0.22	3.39	5.34
Truckee-I80/Truckee River bridge	10/30/1998	1	1.12	1.17	0.63	1.19	2.82
		2	2.27	2.22	7.67	2.12	10.33
		3	—	3.20	2.99	3.02	2.48
		4	4.15	3.92	1.41	4.22	2.68
		5	6.25	—	—	—	—
	12/02/2000	1	1.16	1.23	0.58	1.19	0.93
		2	—	2.13	27.66	1.95	33.12
		3	—	2.96	0.13	3.00	8.14
		4	—	—	—	4.11	4.83
		5	6.12	5.16	0.77	—	—
	08/10/2001	1	1.08	1.17	0.95	1.22	1.63
		2	—	2.42	1.18	2.15	25.71
		3	—	3.15	2.70	3.22	9.21
		4	5.13	4.15	7.02	3.57	34.07
		5	5.88	—	—	—	—

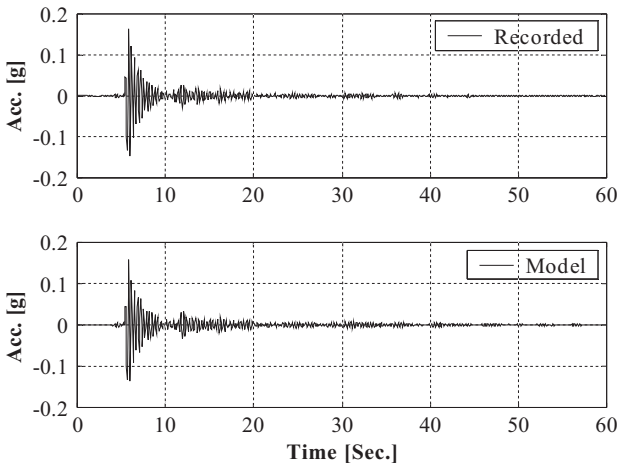

Figure 3. El Centro–Highway 8/Meloland overpass during 04/09/2000 earthquake (channel 7, transverse direction, E–W).

The fundamental frequency of the Ridgecrest–Highway 580/13 Interchange was determined to be 3.39 Hz using the OE method applied to the data from the 03/05/1998 earthquake. As shown in Figure 1, this bridge has four spans with only abutments 1 and 5 and bent 3 instrumented. The SI of this multiple span bridge with few instruments was accordingly shown to be more accurate using the OE method than the ARX method.

The Truckee-I80/Truckee River bridge is one of two relatively large bridges analysed. Several modes were identified from the three events of this bridge. The fundamental frequency was determined to be 1.19 Hz from the first event using the ARX method.

The large size and geometrical configuration (e.g. the expansion joint between bents 5 and 6) of the Sylmar-I5/14 Interchange bridge system (Figure 1) led to the analysis of the bridge in two parts, namely the north and south substructures. The SI results for these substructures are presented separately in Table IV. The fundamental frequency from the 04/11/1999 earthquake data was identified to be 0.74 Hz from the north substructure. On the other hand, the lowest frequency from the south substructure was identified as 0.98 Hz corresponding to the second (anti-symmetric) mode of the whole bridge system. From Table IV, it is noticed that the higher frequencies (>1 Hz) were identifiable from both the north and south substructures. The identified frequencies were lower based on SI using data from the 10/16/1999 earthquake rather than from the 04/11/1999 earthquake. This observation is attributed to the shear key at the expansion joint binding in the first earthquake, which was not the case during the second one. This is supported by the relative motion time histories (transverse displacement, radial direction) between sensors placed on each side of the expansion joint (channels 8 and 12) presented in Figure 4 for the two events. The transverse acceleration (radial direction) time histories from the south substructure (channel 7 in Figure 1) are compared in Figure 5 for the recorded and simulated data using ARX. From this figure, an excellent fit is clear.

The simulation errors of the SI models, summarized in Figure 6, were within acceptable limits. Apart from the ARX analysis on the Ridgecrest–Highway 580/13 Interchange, for

Table IV. Results of linear SI for Sylmar I5/14 Interchange.

Substructure	Earthquake date	Mode #	TFE	OE		ARX	
			ω (Hz)	ω (Hz)	ξ (%)	ω (Hz)	ξ (%)
South	04/11/1999	1	0.98	1.01	3.03	—	—
		2	1.20	1.33	3.22	—	—
		3	1.70	—	—	—	—
		4	2.05	—	—	—	—
		5	2.47	2.21	3.79	—	—
		6	2.78	—	—	—	—
	10/16/1999	1	0.81	0.84	57.16	0.79	11.94
		2	1.01	1.04	13.50	—	—
		3	1.15	—	—	1.28	10.52
		4	1.43	—	—	—	—
		5	1.74	1.64	7.26	1.59	7.64
		6	—	2.05	7.88	2.02	1.46
		7	—	2.39	1.13	2.25	1.86
North	04/11/1999	1	0.70	0.77	0.94	0.74	9.06
		2	1.00	—	—	—	—
		3	1.18	1.20	3.95	1.20	14.43
		4	1.75	1.72	1.57	1.86	2.08
		5	2.05	2.07	1.37	—	—
		6	2.47	—	—	2.52	18.19
		7	2.60	2.60	0.32	2.63	3.48
	10/16/1999	1	0.63	0.60	5.06	0.57	12.41
		2	0.82	0.75	3.46	0.81	4.41
		3	0.98	0.94	2.48	1.07	4.28
		4	1.17	—	—	—	—
		5	1.30	1.31	0.21	1.28	4.23
		6	1.65	1.77	5.29	1.71	1.82
		7	—	1.99	1.60	—	—

reasons mentioned previously, all the multi-input/single-output error values were under 4%. For BART, only the single-input/single-output analysis was performed. The error, although much higher than the multi-input/single-output approach, is still acceptable. In addition to the discussed frequency estimates from the SI, Tables III and IV report damping ratio estimates based on the classical damping assumption.

MODEL PREDICTIONS

As SI aims towards generating a 'pseudo-system', which imitates the 'real-system', the constructed linear models should be able to reasonably predict the structural response from different earthquake data obtained from the same structural system. Spatial variability in large bridge systems and usual low sensor density represent the major deficiency in developing predictive models, as the generated linear models may be too crude to predict the response from

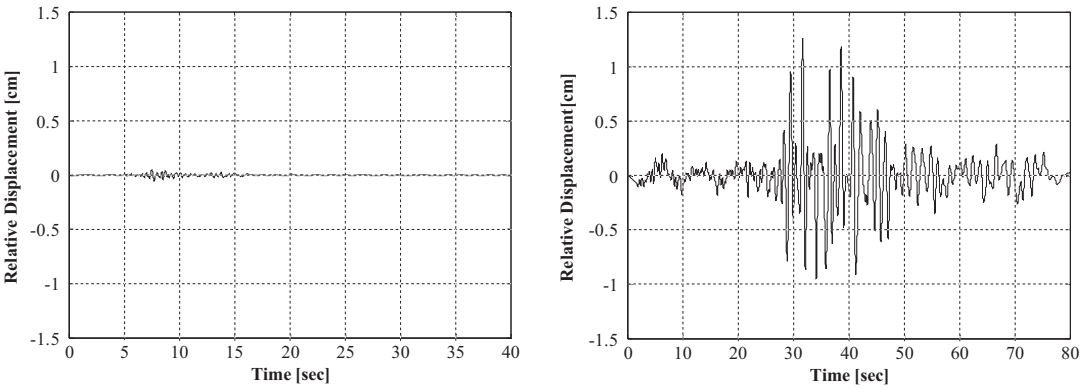

(a) First earthquake of 04/11/1999 (b) Second earthquake of 10/16/1999

Figure 4. Relative displacement in the transverse direction at the expansion joint of Sylmar I5/14 Interchange (between channels 8 and 12, radial direction).

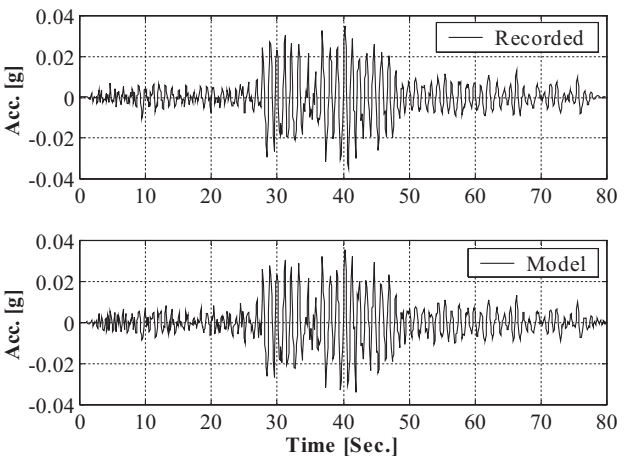

Figure 5. Sylmar I5/14 Interchange (south substructure) during 10/16/1999 earthquake (channel 7, radial direction).

other earthquakes. Another deficiency is the non-linearity that may be present in the system and to which extent it may actually be represented by an equivalent linear model. Moreover, the signal-to-noise ratio of the data is an important factor in determining the predictive accuracy of the models [24].

Prediction of different events for a bridge system using a calibration event has not been investigated before due to limited strong motion data available for bridge systems. The available multiple earthquake recordings for the selected bridges in this study were used to investigate

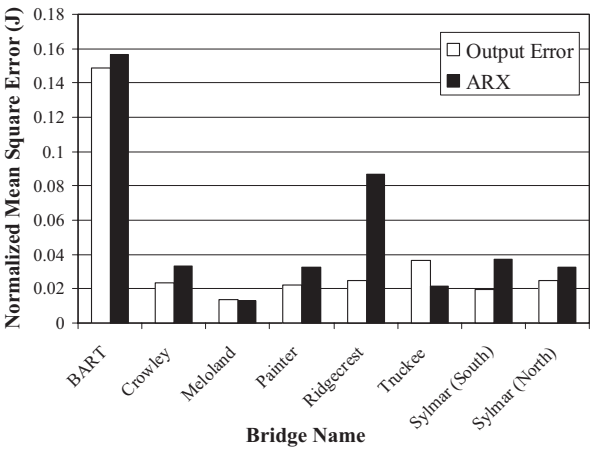

Figure 6. Simulation errors for the different analysed bridges.

the capability of the constructed linear models using calibration events to predict the response from other events. The purpose of constructing such models may be to estimate the time history of the response or simply to determine the maximum acceleration accurately. These models can also be used to understand how to represent the behaviour of specific elements in a bridge system. More importantly, future use of such models to detect damage in systems with dense sensor array can be performed by comparing the behaviour of the predictive models with the recorded data.

Two of the recorded events for the Truckee I-80/Truckee River bridge (see Table II) were used to test the prediction capabilities of the linear models. Because the bridge did not have base acceleration sensors, the boundary conditions were not well defined. Accordingly, the free-field motion, which was near the east abutment of the bridge, was used along with the bridge deck recordings for SI. The linear ARX models had J of 2.2 and 1.68% for the 10/30/1998 and 12/02/2000 events, respectively. Application of the model from the first event to the second gave the time history comparison for channel 7 (E–W direction) shown in Figure 7(a) with $J = 13.8\%$. Using the model from the second event to predict the deck acceleration of the first event is shown in Figure 7(b) with $J = 12.8\%$. The error values of both predictions are close and acceptable. The spatial extent of the bridge and the scarcity of sensors also render the results adequate.

The data from the three earthquakes of the Lake Crowley–Highway 395 bridge (see Table II), were used to test model predictability. The event on 06/08/1998 was used initially as a calibration model using ARX where $J = 4.4\%$ to predict the other two events on 06/14/1998 and 05/15/1999. Using this model, the predicted deck transverse acceleration (E–W direction, channel 7) had J values of 6.8 and 10.1% for the second and third events, respectively. The results are shown in Figures 8(a) and 8(b). The model from the third event was also used to predict the first and second events. The sixth-order ARX model formed for the third event with $J = 3.6\%$ predicted the first two events, Figures 8(c) and 8(d), with J values of 11.2 and 29.5%, respectively. In this latter prediction, the error in the second event is high but still

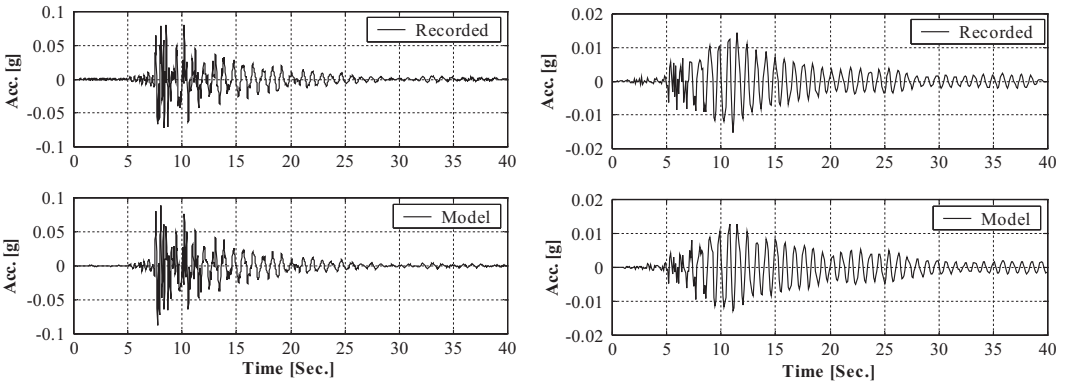

(a) Predicted 30/10/1998 event using model from 12/02/2000 event

(b) Predicted 12/02/2000 event using model from 30/10/1998 event

Figure 7. Model prediction from Truckee I-80/Truckee River bridge data (channel 7, transverse direction, E–W).

within acceptable limits. Accordingly, the model from the first event was more successful in predicting other events.

The Rio Dell–Highway 101/Painter Street overpass is an important case for the demonstration of model predictions as the recorded ground motions of this bridge were of different intensity, as listed in Table II. As shown in the linear SI results, the fundamental frequency of the bridge reduced considerably in the third earthquake. Using a sixth-order ARX model from the 11/21/1986 event with $J = 3.9\%$, the events of 07/31/1987 and 04/25/1992 were predicted with J values of 17.9 and 14.5%, respectively. The time history results for transverse acceleration at channel 7 (N–S direction) are shown in Figure 9. Based on the normalized mean square error J, the third event was better predicted by this model and the fit was acceptable considering that the peak mid-deck acceleration reached 0.9g during the third event.

RECURSIVE FILTER ESTIMATIONS

The modal frequencies of the bridge systems were determined using linear ARX and OE filters in the previous sections. The procedure was successful in obtaining excellent time fits for the recorded motions. Although this was the case, it should be noted that the obtained frequencies for bridges with non-linear behaviour were based on linear models. For estimation of the frequency change with time in such bridges, recursive filters were employed. The Rio Dell–Highway 101/Painter Street overpass, which experienced high deck acceleration close to 1.1g during the 04/25/1992 event (Cape Mendocino-Petrolia earthquake) and a deck acceleration close to 0.3g for the 07/31/1987 event, was the right candidate for this recursive estimation. As shown in Table III, the linear SI of this bridge revealed a reduction of the fundamental frequency for the 04/25/1992 event with a relatively high damping ratio. It is worth mentioning that the linear models gave good fit to the time history indicating that

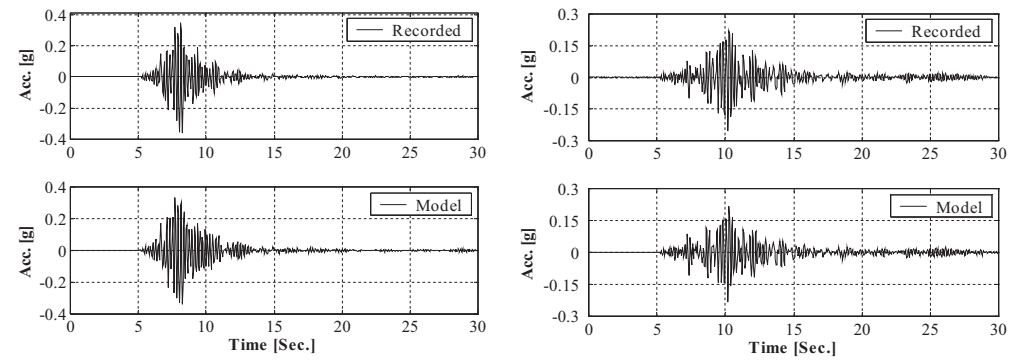

(a) Predicted 06/14/1998 event using model from 06/08/1998 event

(b) Predicted 05/15/1999 event using model from 06/08/1998 event

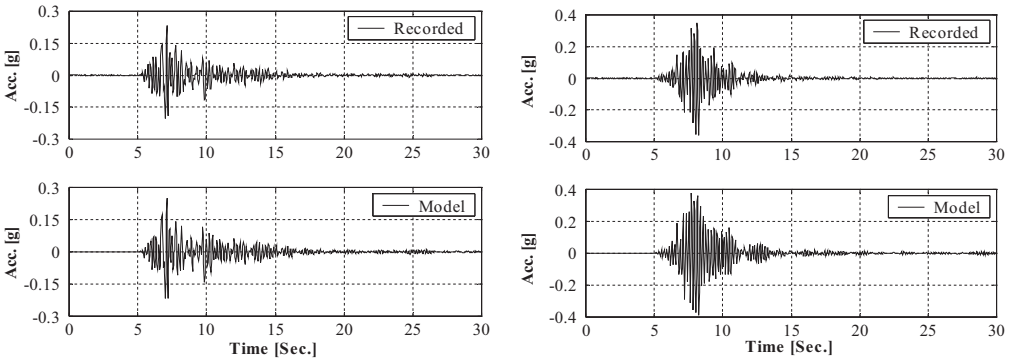

(c) Predicted 06/08/1998 event using model from 05/15/1999 event

(d) Predicted 06/14/1998 event using model from 05/15/1999 event

Figure 8. Model prediction from Lake Crowley–Highway 395 bridge data (channel 7, transverse direction, E–W).

the probable change of properties due to damage of the bridge did not affect the model significantly, which was unexpected for a system undergoing such high acceleration.

In the application of the recursive filter, it is expected that the model order and the corresponding error would be lower than those of the linear filter. As shown in Figure 10 for the 07/31/1987 event of the Rio Dell–Highway 101/Painter Street overpass, the prediction error for the model has an optimal order of 2 or 3. The reported error in this case is the normalized prediction error (NPE) with respect to the recorded output $y(t)$. The evolution of the frequency is given in Figures 11(a) and 11(b) for models of orders 2 and 3, respectively. The second-order model with different forgetting factor λ stabilized at a value of 4.65 Hz whereas the third-order model stabilized with some oscillations at 4.45 Hz. This indicates that frequency estimates from recursive filters are sensitive to model order not to the value of λ for the linear response cases. In addition, the NPE was not a sufficient criterion to select the model order as evident from the oscillations in the third-order model.

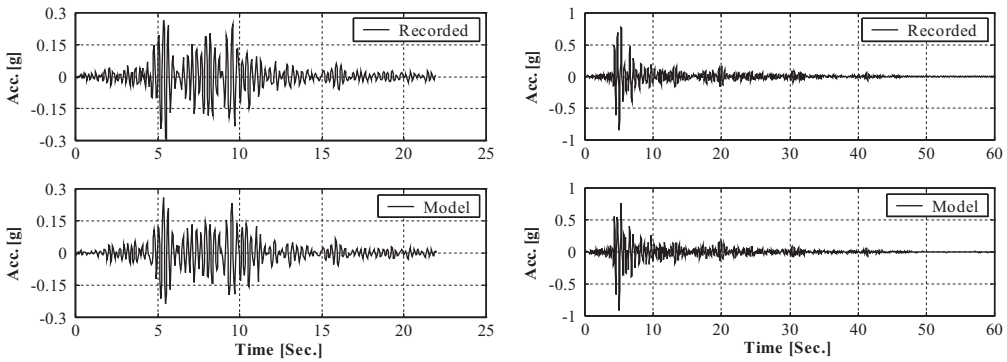

(a) Predicted 07/31/1987 event using model from 11/21/1986 event

(b) Predicted 04/25/1992 event using model from 11/21/1986 event

Figure 9. Model prediction from the Rio Dell–Highway 101/Painter Street overpass data (channel 7, transverse direction, N–S).

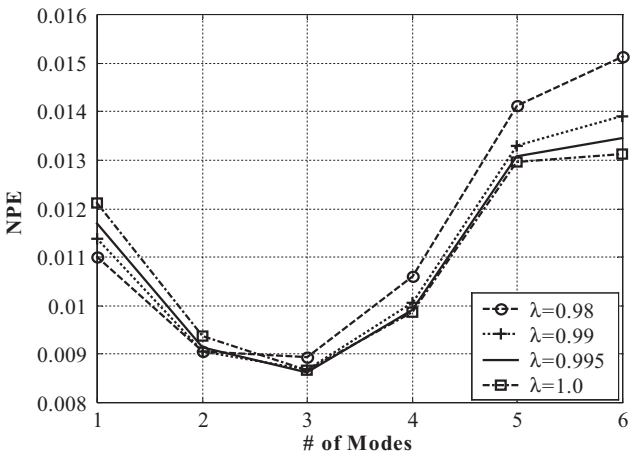

Figure 10. Variation of simulation error for 07/31/1987 event of the Rio Dell–Highway 101/Painter Street overpass.

The variations of the NPE with the model order for different forgetting factors λ are presented in Figure 12 for the 04/25/1992 earthquake where NPE increases with decreasing λ for higher number of modes involved in the estimation. From an error stand point, it was concluded that the first- or second-order models were optimum in this case. For a first-order model, the frequency variation is given in Figure 13(a). The model cannot capture the highly damped first mode at approximately 3 Hz due to dominance of the second mode and due to model deficiency for the input–output sensor arrangement. The second mode was

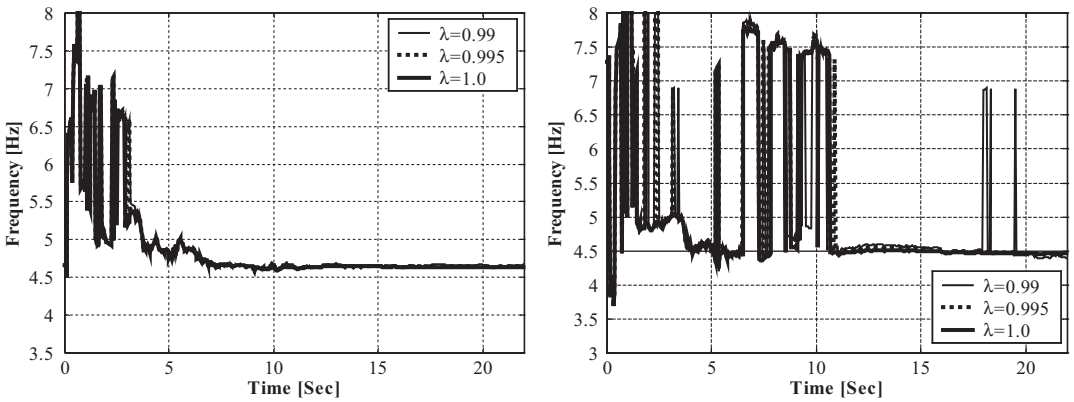

Figure 11. Evolution of frequency with time for 07/31/1987 event of the Rio Dell–Highway 101/Painter Street overpass.

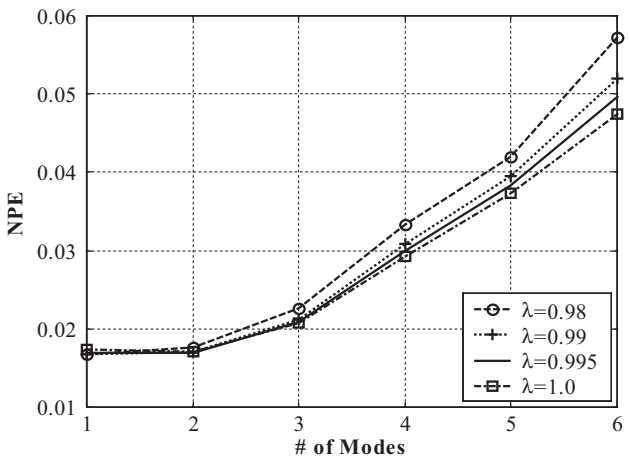

Figure 12. Variation of normalized prediction error for 04/25/1992 event of the Rio Dell–Highway 101/Painter Street overpass.

predicted well with frequency changing towards 4 Hz. Reducing λ to 0.98 affected the stability of the frequency estimate. Therefore, it was decided that λ values of 0.99 or 0.995 were more dependable. The model with $\lambda = 0.995$ converged to 4.19 Hz, whereas with $\lambda = 0.99$, it converged to 3.95 Hz. The damping ratio variations are given in Figure 13(b) where also the model with $\lambda = 0.98$ failed to stabilize. Models with λ values of 0.99, 0.995 and 1.00 converged to damping ratios of 20, 16 and 12%, respectively.

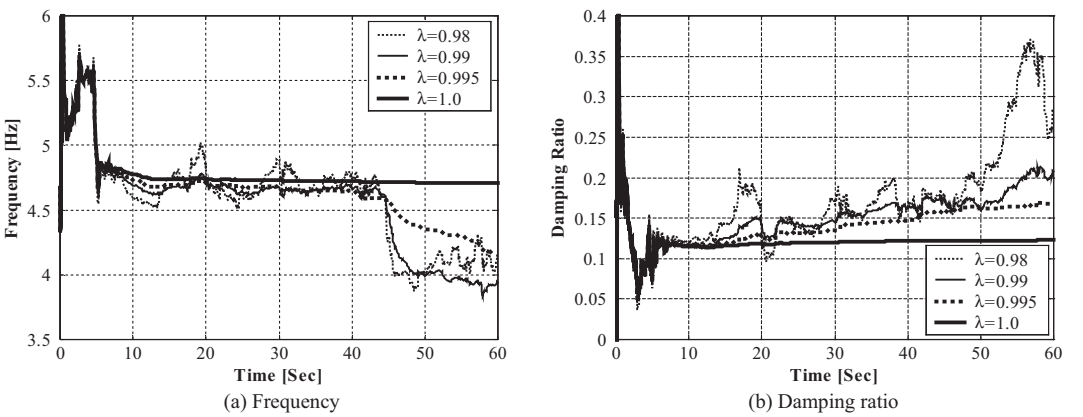

(a) Frequency (b) Damping ratio

Figure 13. Evolution of properties with time for 04/25/1992 event of the Rio Dell–Highway 101/Painter Street overpass using the accelerometer T-layout of Figure 2(a).

The dominance of the second mode for the 04/25/1992 earthquake response can be attributed to model deficiency and dependency of the bridge modal properties on ground motion as the boundary conditions change. As most of the analysed bridge systems had fixed support conditions, the T-system of Figure 2(a) enabled an efficient sensor arrangement to define the system and to determine the fundamental frequencies. However, for Painter Street overpass during the 04/25/1992 event, the ground motion at the west abutment reached 1.3g whereas at the deck sensor near the abutment, the acceleration was 1.1g. This is indicative that the deck did not behave as being fixed at the west abutment. Accordingly, the T-system in Figure 2(a), used for SI, was deficient in this case. The input–output identification scheme was changed to effectively capture the fundamental frequency where a two input recursive model was constructed as shown in Figure 2(b). This scheme was more effective in determining the fundamental frequency with a first-order recursive ARX filter. As shown in Figure 14(a), the fundamental frequency changed from 3.45 Hz to 3.25 Hz for $\lambda = 0.99$ with slight differences between the results for different λ values. The accuracy was relatively low with NPE = 10.6% because of using fewer sensors in this new scheme of Figure 2(b). The damping values given in Figure 14(b) are quite high with significant differences depending on the value of the forgetting factor λ.

PRACTICAL IMPLICATIONS

In addition to the SI methodology and results presented in previous sections, current practices of bridge modelling for the purpose of determining the modal properties were evaluated and results were compared with the obtained frequencies from the SI. The evaluation was performed through finite-element analyses of the investigated seven bridge systems with emphasis on modelling assumptions, especially abutment stiffness using linear springs. In general, current practices proved adequate with reservations on the need for proper modelling of connections.

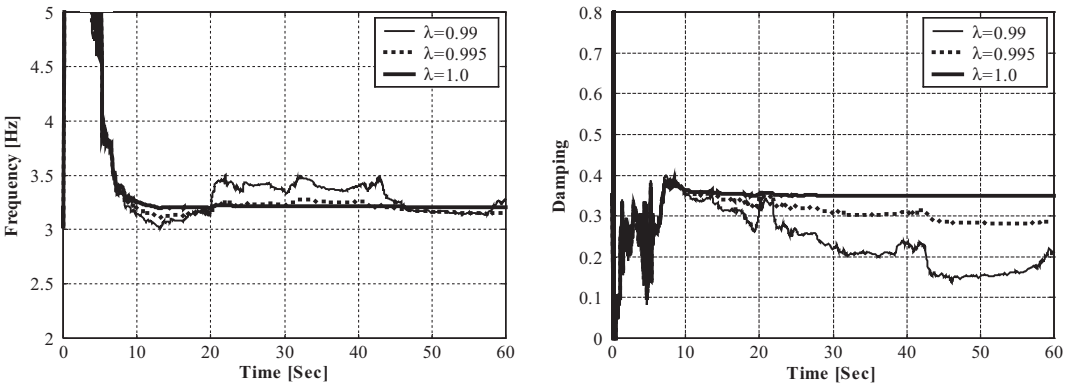

(a) Frequency (b) Damping ratio

Figure 14. Evolution of properties with time for 04/25/1992 event of the Rio Dell–Highway 101/Painter Street overpass using the two input model of Figure 2(b).

For large bridges with multiple spans and tall columns, the effect of abutment characteristics was not critical but cracked moment of inertia of approximately 40% of the gross moment of inertia for the columns had to be considered for accurate estimates of the modal frequencies. For small systems (e.g. two span systems), assuming column stiffness based on gross moment of inertia was adequate. Finally, special attention has to be given to modelling of expansion joints.

CONCLUDING REMARKS

The study focused on the estimation of the modal frequencies of seven instrumented bridges in California. These bridges were selected to have a diverse sample with different configurations of structural systems. Linear system identification was carried out using discrete time-invariant filters in the form of ARX and OE to a specific multi-input/single-output instrumentation scheme (Figure 2(a)). Excellent time domain fits were obtained even for high ground motion acceleration as in the Rio Dell–Highway 101/Painter Street overpass. The estimated linear models were also used for the purpose of prediction. The prediction models, which imitate the system behaviour, were tested for three bridge systems giving reasonably accurate predictions with acceptable normalized mean square errors. The importance of the selection of the calibration event was deduced to be instrumental in obtaining good predictions from such models.

Recursive filters were used on the Rio Dell–Highway 101/Painter Street overpass to investigate the change of the system behaviour. Although definite change in the system was detected for the high intensity event, parameter (such as the forgetting factor) dependency for the used method was discussed. Therefore, such parameters have to be carefully selected. The deficiency of the selected T-scheme input–output arrangement (Figure 2(a)) was pronounced in the results for recursive filters. Recursive filters based on a different set of input–output

arrangement (Figure 2(b)) were more reliable in capturing the fundamental mode of vibration due to changes in boundary conditions.

ACKNOWLEDGEMENTS

The authors gratefully acknowledge the financial support provided by the California Strong Motion Instrumentation Program under the Contract No. 1098-714 with funding from the California Department of Conservation.

REFERENCES

1. Hipley P, Huang M, Shakal A. Bridge instrumentation and post-earthquake evaluation of bridges. *SMIP98 seminar on utilization of strong motion data*, Sacramento, CA, U.S.A., 1998; 53–71.
2. Werner SD, Beck JL, Levine MB. Seismic response evaluation of Meloland Road overpass using 1979 Imperial Valley earthquake records. *Earthquake Engineering and Structural Dynamics* 1987; **15**:249–274.
3. Werner SD, Crouse CB, Katafygiotis LS, Beck JL. Use of strong motion records for model evaluation and seismic analysis of a bridge structure. *Proceedings of the Fifth U.S. National Conference on Earthquake Engineering*, Chicago, IL, U.S.A., vol. 1, 1994; 511–520.
4. Wilson JC, Tan BS. Bridge abutments: assessing their influence on earthquake response of Meloland Road overpass. *Journal of Engineering Mechanics* (ASCE) 1990; **116**(8):1838–1856.
5. Wilson JC. Analysis of the observed seismic response of a highway bridge. *Earthquake Engineering and Structural Dynamics* 1986; **14**:339–354.
6. Safak E. Use of structural response data from small earthquakes and aftershocks. *Proceedings of the 26th Joint Meeting of U.S.–Japan Cooperative Program in Natural Resources Panel on Wind and Seismic Effects*, NIST SP 871, Gaithersburg, Maryland, 1994; 613–623.
7. Levine MB, Scott RF. Dynamic response verification of simplified bridge-foundation model. *Journal of Geotechnical Engineering* (ASCE) 1989; **115**(2):246–260.
8. Fenves GL, Desroches R. Response of the northwest connector in the Landers and Big Bear earthquakes. *Report No.* 94/12, Earthquake Engineering Research Center, University of California, Berkeley, 1994.
9. Abdel-Ghaffar AM, Niazy AM, Masi SF. Analysis of the seismic records of a suspension bridge. *Proceedings of the ASCE Structural Congress '93*, New York, vol. 2, 1993; 1509–1514.
10. Lus H, Betti R, Longman RW. Identification of linear structural systems using earthquake induced vibration data. *Earthquake Engineering and Structural Dynamics* 1999; **28**:1449–1467.
11. Saadeghvaziri MA, Foutch DA. Effects of vertical motion on the inelastic behavior of highway bridges. *Proceedings of the ASCE Structural Congress '89*, New York, 1989; 51–61.
12. Tseng WS, Yang MS, Penzien J. Seismic performance investigation of the Hayward BART elevated section. *Data Utilization Report* CSMIP/92-02, 1992.
13. Fenves GL, Filippou FC, Sze D. Response of the Dumbarton bridge in the Loma Prieta earthquake. *Report No.* 92/02, Earthquake Engineering Research Center, University of California, Berkeley, 1992.
14. Desroches R, Fenves GL. Evaluation of recorded earthquake response of a curved highway bridge. *Earthquake Spectra* 1997; **13**(3):363–386.
15. Goel RK, Chopra AK. Seismic response study of the Hwy 101/Painter Street overpass near Eureka using strong-motion records. *Data Utilization Report CSMIP*/95-01, 1995.
16. McCallen DB, Romstadt KM. Dynamic analysis of a skewed short span box girder overpass. *Earthquake Spectra* 1994; **10**(4):729–755.
17. Tsai NC, Firouz A, Sedarat H, Nisar A, Werner SD. Application of Caltrans current seismic evaluation procedures to selected short bridge overcrossing structures. *Technical Report*, Dames and Moore, 1993.
18. Chaudhary MTA, Abe M, Fujino Y, Yoshida J. System identification of two base-isolated bridges using seismic records. *Journal of Structural Engineering* (ASCE) 2000; **126**(10):1187–1195.
19. Loh CH, Lee ZK. Seismic monitoring of a bridge: assessing dynamic characteristics from both weak and strong ground motions. *Earthquake Engineering and Structural Dynamics* 1997; **26**:269–288.
20. Safak E. Identification of linear structures using discrete-time filters. *Journal of Structural Engineering* (ASCE) 1991; **117**(10):3064–3085.
21. Glaser SD. System identification and its application to soil dynamics. *Report No.* 98/01, Geotechnical Engineering, University of California, Berkeley, 1998.

22. Shinozuka M, Ghanem R. Structural system identification 2: experimental verification. *Journal of Engineering Mechanics* (ASCE) 1995; **121**(2):265–273.
23. Loh CH, Lin HM. Application of off-line and on-line identification techniques to building seismic response data. *Earthquake Engineering and Structural Dynamics* 1996; **25**:269–290.
24. Glaser SD, Baise LG. System identification estimation of soil properties at the Lotung site. *Soil Dynamics and Earthquake Engineering* 2000; **19**:521–531.
25. Chopra AK. *Dynamics of Structures.* Prentice-Hall: New Jersey, 1995.
26. Ljung L. System identification toolbox users guide. Math Works, Inc: Natick, MA, 1997.
27. Maroney BM, Romstadt KM, Chajes MJ. Interpretation of Rio Dell freeway response during six recorded earthquake events. *Proceedings of the Fourth U.S. National Conference on Earthquake Engineering*, Palm Springs, CA, U.S.A., vol. 1, 1990; 1007–1016.

